A structure for ultra long span unrepeatered optical transmission systems

Hao Ruan (阮 浩) and Chaoqin Gan (甘朝钦)*

Key Lab of Specialty Fiber Optics and Optical Access Network, Shanghai University, Shanghai 200072, China

**E-mail: cqgan@shu.edu.cn*

Received September 25, 2009

A novel structure for ultra long span optical transmission systems is proposed. In the scheme, the inverse fast Fourier trans form (IFFT) is used as a way of inverse multiplexing. A 40-Gb/s (total effective capacity) system based on the proposed scheme is simulated to evaluate its performance without consideration for dispersion compensation. Simulation results indicate that the proposed system can tolerate distortion caused by chromatic dispersion effectively after long distance transmission.

OCIS codes: 060.0060, 060.2360, 060.4080.

doi: 10.3788/COL20100806.0564.

Ultra long span (ULS) optical transmission systems are not only an enabling technology, but also an effective solution for special circumstances: regional non-relay network, hybrid networking for undersea relay systems, hybrid networking for terrestrial transmission systems, etc. Extending span distance is an important way to reduce the cost of long haul dense wavelength division multiplexing (DWDM) systems. There has been interest in lowering operating costs for terrestrial and submarine systems by increasing the length of the transmission spans, thereby reducing the number of repeater sites[1].

To make the span length longer is of prime necessity for an ULS unrepeatered system. Efforts have been made and some schemes were proposed[2−5]. In these schemes, researchers optimized the configuration of optical amplifiers and fiber[2,3] or used an advanced modulation format to achieve the goal[4,5]. With the increase of bit rate of the system, chromatic dispersion becomes a great impediment in optical transmission systems. How to tackle with dispersion and achieve long span distance is the problem that must be solved in commercial long fiber span systems.

A structure for ULS unrepeatered transmission system is presented in this letter. In the proposed system, 4-quadrature amplitude modulation (QAM) and 8-inverse fast fourier transform (IFFT) are used to generate transmitted signals. Return-to-zero (RZ) and three-level formats are used in the transmission. A 40-Gb/s (total effective capacity) system based on the proposed scheme is simulated under the condition of not considering dispersion compensation. We will show that the proposed system can tolerate more distortion due to dispersion than RZ systems. Even without dispersion compensation and Raman amplification, a quality factor (Q-factor) of 9.5 can be obtained after 95-km single span unrepeatered transmission.

The transmitter configuration shown in Fig. 1 is used in the investigation. The data are first mapped to generate QAM symbols (constellation). Symbols are then assigned to the inputs of IFFT. Here, the inputs are represented by X which are constrained to have Hermitian symmetry:

$$\begin{cases} X^*(k) = X(N-k) \quad k = 2n+1, \\ \qquad\qquad\qquad\qquad n = 0, 1, \cdots, \frac{N}{2}-1 \\ X(k) = 0 \qquad\quad k = 2n, \;\; n = 0, 1, \cdots, \frac{N}{2}-1 \end{cases}, \qquad (1)$$

where N is the size of the IFFT. The outputs of IFFT are

$$x(n) = \text{IFFT}\,[X(k)] = \frac{1}{N}\sum_{k=0}^{N-1} X(k)\mathrm{e}^{\mathrm{j}\frac{2\pi}{N}kn}, \qquad (2)$$

The transmitted signals are clipped from $x(n)$ as

$$x_{\mathrm{c}}(n) = \begin{cases} x(n) & x(n) > 0 \\ 0 & x(n) < 0 \end{cases}. \qquad (3)$$

The feasibility of recovering constellation on the receiver side by transmitting $x_{\mathrm{c}}(n)$ has already been verified[6]. Generally, the value of each components of x_{c} is arbitrary. In the following, analysis is given to show that RZ and three-level formats can be used to be transmission formats in the fiber.

Since X obeys Hermitian symmetry, components of x are real numbers and we can derive

$$\begin{aligned} Nx(n) &= X(1)\mathrm{e}^{\mathrm{j}\frac{2\pi}{N}n} + X(3)\mathrm{e}^{\mathrm{j}\frac{2\pi}{N}3n} + \cdots + X(N-3)\mathrm{e}^{\mathrm{j}\frac{2\pi}{N}(N-3)n} + X(N-1)\mathrm{e}^{\mathrm{j}\frac{2\pi}{N}(N-1)n} \\ &= X(1)\mathrm{e}^{\mathrm{j}\frac{2\pi}{N}n} + X(3)\mathrm{e}^{\mathrm{j}\frac{2\pi}{N}3n} + \cdots + X^*(3)\mathrm{e}^{\mathrm{j}\frac{2\pi}{N}(N-3)n} + X^*(1)\mathrm{e}^{\mathrm{j}\frac{2\pi}{N}(N-1)n} \\ &= [X(1)\mathrm{e}^{\mathrm{j}\frac{2\pi}{N}n} + X^*(1)\mathrm{e}^{\mathrm{j}\frac{2\pi}{N}(N-1)n}] + [X(3)\mathrm{e}^{\mathrm{j}\frac{2\pi}{N}3n} + X^*(3)\mathrm{e}^{\mathrm{j}\frac{2\pi}{N}(N-3)n}] + \cdots \\ &\quad + [X(\frac{N}{2}-1)\mathrm{e}^{\mathrm{j}\frac{2\pi}{N}(\frac{N}{2}-1)n} + X^*(\frac{N}{2}-1)\mathrm{e}^{\mathrm{j}\frac{2\pi}{N}(\frac{N}{2}+1)n}] \\ &= |X(1)|\,\mathrm{e}^{\mathrm{j}(\varphi_1+\frac{2\pi}{N}n)} + |X(1)|\,\mathrm{e}^{-\mathrm{j}(\varphi_1+\frac{2\pi}{N}n)} + |X(3)|\,\mathrm{e}^{\mathrm{j}(\varphi_3+\frac{2\pi}{N}3n)} + |X(3)|\,\mathrm{e}^{-\mathrm{j}(\varphi_3+\frac{2\pi}{N}3n)} + \cdots \end{aligned}$$

$$+\left|X(\frac{N}{2}-1)\right|\mathrm{e}^{\mathrm{j}[\varphi_{\frac{N}{2}-1}+\frac{2\pi}{N}(\frac{N}{2}-1)n]}+\left|X(\frac{N}{2}-1)\right|\mathrm{e}^{-\mathrm{j}[\varphi_{\frac{N}{2}-1}+\frac{2\pi}{N}(\frac{N}{2}-1)n]}$$
$$=2\left|X(1)\right|\cos(\varphi_1+\frac{2\pi}{N}n)+2\left|X(3)\right|\cos(\varphi_3+\frac{2\pi}{N}3n)+\cdots+2\left|X(\frac{N}{2}-1)\right|\cos[\varphi_{\frac{N}{2}-1}+\frac{2\pi}{N}(\frac{N}{2}-1)n], \quad (4)$$

where φ_k is the phase of $X(k)$. $x\,(n)$can be expressed as

$$x(n)=\frac{2}{N}\Big\{\left|X(1)\right|\cos(\varphi_1+\frac{2\pi}{N}n)+\left|X(3)\right|\cos(\varphi_3+\frac{2\pi}{N}3n)+\cdots+\left|X(\frac{N}{2}-1)\right|\cos[\varphi_{\frac{N}{2}-1}+\frac{2\pi}{N}(\frac{N}{2}-1)n]\Big\}. \quad (5)$$

Only when 4-QAM and 8-IFFT are used, there is

$$\left|X(1)\right|=\left|X(3)\right|, \quad (6)$$

$$x(n)=\frac{\sqrt{2}}{4}[\cos(\varphi_1+\frac{\pi}{4}n)+\cos(\varphi_3+\frac{\pi}{4}3n)], \quad (7)$$

where φ_1 and φ_3 are confined to $\pm\frac{\pi}{4}$ and $\pm\frac{3\pi}{4}$, respectively.

A property can be drawn from Eqs. (3) and (7). When n is an even number, $x_{\mathrm{c}}(n)$ has only two different values: 0 and $\frac{1}{2}$. When n is an odd number, $x_{\mathrm{c}}(n)$ has only three different values: 0, $\frac{\sqrt{2}}{2}$, and $\frac{\sqrt{2}}{4}$.

Components of x_{c} are then reshaped by setting corresponding threshold in decision device. For even channels, RZ electrical waveform is generated by using high voltage to represent "$\frac{1}{2}$" and zero voltage to represent "0". Here, V_m is used to represent the amplitude of high voltage. For odd channels, three-level electrical waveform is generated by using high voltage V_m to represent "$\frac{\sqrt{2}}{2}$", voltage $\frac{V_m}{2}$ to represent "$\frac{\sqrt{2}}{4}$", and zero voltage to represent "0". The electrical waveforms of eight channels directly drive the $\mathrm{LiNbO_3}$ intensity-modulators to produce optical signals. The lightwave of eight channels are then coupled into the fiber.

At the receiver terminal shown in Fig. 2, the light in each channel is firstly detected. After being filtered, the electrical waveforms of eight channels are synchronized and sampled at the peak of received pulses. The voltage values of samples of eight tributaries in parallel form the vector x_{r}. When the system is supposed to be linear, x_{r} can be expressed as

$$\begin{bmatrix} x_{\mathrm{r}}(0)\\ x_{\mathrm{r}}(1)\\ x_{\mathrm{r}}(2)\\ x_{\mathrm{r}}(3)\\ x_{\mathrm{r}}(4)\\ x_{\mathrm{r}}(5)\\ x_{\mathrm{r}}(6)\\ x_{\mathrm{r}}(7)\end{bmatrix}=A\begin{bmatrix} \frac{x_{\mathrm{c}}(0)}{0.5}V_m\\ \frac{x_{\mathrm{c}}(1)}{0.7071}V_m\\ \frac{x_{\mathrm{c}}(2)}{0.5}V_m\\ \frac{x_{\mathrm{c}}(3)}{0.7071}V_m\\ \frac{x_{\mathrm{c}}(4)}{0.5}V_m\\ \frac{x_{\mathrm{c}}(5)}{0.7071}V_m\\ \frac{x_{\mathrm{c}}(6)}{0.5}V_m\\ \frac{x_{\mathrm{c}}(7)}{0.7071}V_m\end{bmatrix}+\begin{bmatrix} d(0)\\ d(1)\\ d(2)\\ d(3)\\ d(4)\\ d(5)\\ d(6)\\ d(7)\end{bmatrix}=A\cdot V_m\begin{bmatrix} \frac{x_{\mathrm{c}}(0)}{0.5}\\ \frac{x_{\mathrm{c}}(1)}{0.7071}\\ \frac{x_{\mathrm{c}}(2)}{0.5}\\ \frac{x_{\mathrm{c}}(3)}{0.7071}\\ \frac{x_{\mathrm{c}}(4)}{0.5}\\ \frac{x_{\mathrm{c}}(5)}{0.7071}\\ \frac{x_{\mathrm{c}}(6)}{0.5}\\ \frac{x_{\mathrm{c}}(7)}{0.7071}\end{bmatrix}+\begin{bmatrix} d(0)\\ d(1)\\ d(2)\\ d(3)\\ d(4)\\ d(5)\\ d(6)\\ d(7)\end{bmatrix}, \quad (8)$$

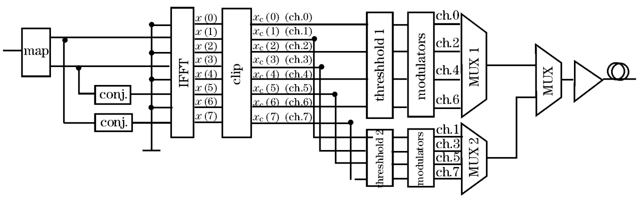

Fig. 1. Configuration of the transmitter. MUX: multiplexer; conj.: conjugate.

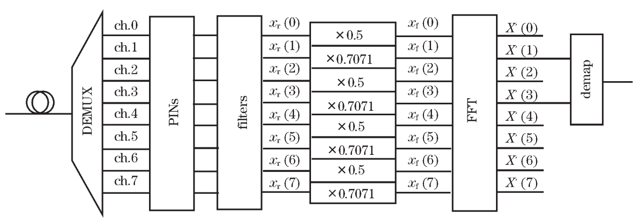

Fig. 2. Configuration of the receiver.

where A is an attenuation coefficient and $d\,(k)$ represent the distortion. Each component of x_{r} should be multiplied by a corresponding coefficient. For even channels, the coefficient is "$\frac{1}{2}$". For odd channels, the coefficient is "$\frac{\sqrt{2}}{2}$". x_{f} is used to represent the inputs of fast fourier transform (FFT). Because

$$\begin{cases} x_{\mathrm{f}}(0)=x_{\mathrm{r}}(0)\times 0.5\\ x_{\mathrm{f}}(1)=x_{\mathrm{r}}(1)\times 0.7071\\ x_{\mathrm{f}}(2)=x_{\mathrm{r}}(2)\times 0.5\\ x_{\mathrm{f}}(3)=x_{\mathrm{r}}(3)\times 0.7071\\ x_{\mathrm{f}}(4)=x_{\mathrm{r}}(4)\times 0.5\\ x_{\mathrm{f}}(5)=x_{\mathrm{r}}(5)\times 0.7071\\ x_{\mathrm{f}}(6)=x_{\mathrm{r}}(6)\times 0.5\\ x_{\mathrm{f}}(7)=x_{\mathrm{r}}(7)\times 0.7071\end{cases}, \quad (9)$$

we can get

$$\begin{bmatrix} x_\mathrm{f}(0) \\ x_\mathrm{f}(1) \\ x_\mathrm{f}(2) \\ x_\mathrm{f}(3) \\ x_\mathrm{f}(4) \\ x_\mathrm{f}(5) \\ x_\mathrm{f}(6) \\ x_\mathrm{f}(7) \end{bmatrix} = A \cdot V_m \begin{bmatrix} x_\mathrm{c}(0) \\ x_\mathrm{c}(1) \\ x_\mathrm{c}(2) \\ x_\mathrm{c}(3) \\ x_\mathrm{c}(4) \\ x_\mathrm{c}(5) \\ x_\mathrm{c}(6) \\ x_\mathrm{c}(7) \end{bmatrix} + \begin{bmatrix} d(0)\times 0.5 \\ d(1)\times 0.7071 \\ d(2)\times 0.5 \\ d(3)\times 0.7071 \\ d(4)\times 0.5 \\ d(5)\times 0.7071 \\ d(6)\times 0.5 \\ d(7)\times 0.7071 \end{bmatrix} = A \cdot V_m \begin{bmatrix} x_\mathrm{c}(0) \\ x_\mathrm{c}(1) \\ x_\mathrm{c}(2) \\ x_\mathrm{c}(3) \\ x_\mathrm{c}(4) \\ x_\mathrm{c}(5) \\ x_\mathrm{c}(6) \\ x_\mathrm{c}(7) \end{bmatrix} + \begin{bmatrix} d'(0) \\ d'(1) \\ d'(2) \\ d'(3) \\ d'(4) \\ d'(5) \\ d'(6) \\ d'(7) \end{bmatrix}. \quad (10)$$

Thus, the outputs of FFT can be expressed as

$$X_\mathrm{r}(k) = \mathrm{FFT}\left[x_f(n)\right] = AV_m \cdot \mathrm{FFT}\left[x_\mathrm{c}(n)\right] + \mathrm{FFT}\left[d'(n)\right] = AV_m \cdot X'(k) + D'(k), \quad (11)$$

where X' is the fast Fourier transform of x_c. When k is odd, there is a relationship between $X'(k)$ and $X(k)$:

$$X'(k) = \frac{1}{2} X(k). \quad (12)$$

The components of X' on even subcarriers are noise[7]. Therefore, the constellation can be recovered by $X'(1)$ and $X'(3)$, and values on even subcarriers are discarded.

This scheme can be seen as a novel way of inverse multiplexing. Traditional inverse multiplexing is always realized by means of optical time division multiplexing (OTDM). Unrepeatered span length can be extended by inverse multiplexing when the bit rate is not too high. In case of bit rate higher than 40 Gb/s, time-delay control in inverse multiplexing is too complicated to overcome. Cache in the system can also be a problem. Instead of inverse multiplexing enabled by OTDM, the proposed scheme processes high speed data through constellation mapping. Constellation is used to do IFFT. The output data of 8-IFFT form eight tributaries of transmitting signals in parallel. The bit rate of each tributary is lower than that of the system. In this way, inverse multiplexing in high speed optical transmission can be realized with no consideration to time-delay control and cache.

As shown in Eq. (1), because there exists conjugation relationship among the inputs of 8-IFFT, the bit rate of each tributary is a quarter of that of the system. Thus the chromatic dispersion and nonlinearity effect can be easily tackled in the transmission fiber. Unrepeatered span length of the system can be lengthened effectively.

Two different amplitude modulated formats are deployed in the system. For even channels, RZ formats are used and the electrical waveform (ch.0) used to drive the optical modulator is shown in Fig. 3(a). For odd channels, three-level formats are used and the electrical waveform (ch.1) used to drive the optical modulator is shown Fig. 3(b).

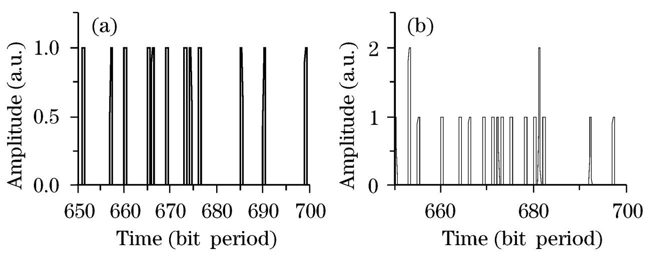

Fig. 3. Electrical waveform of (a) ch.0 and (b) ch.1.

We know that high-order optical modulation format, especially 16-ary QAM, is regarded as a promising candidate for future high capacity and high spectral efficiency optical transmission systems[8]. However, when multi-level modulation is used, threshold can be greatly affected by distortion at the receiver and thus the bit error rate (BER) increases. When phase modulation is performed, modulation and receiver setup is so complicated that the cost goes up. For the proposed system, though three-level format is deployed, threshold decision is not used. There is no need to decide "1" or "0" at the receiver by setting threshold. Transmitting data are recovered by the voltage of samples through electrical processing. Since some deviation of voltage is allowed, the system has a good tolerance to waveform distortion.

In order to study the transmission performance of the system and demonstrate its feasibility, a simulation is performed with OptiSystem. A 40-Gb/s (total effective capacity) system is simulated. The number of simulated bits is equal to 2^{13}. The wavelength division multiplexing (WDM) signals are generated by eight continuous-wave (CW) lasers emitting in the C-band (193.1−193.8 THz) with a channel spacing of 100 GHz. Thanks to the electrical processing in the transmitter, the bit rate of each WDM channel becomes 10 Gb/s. The lightwave of 8 channels are coupled into a +20 dBm post-amplifier. The fiber is linear and purely dispersive, with a typical dispersion value of G.652 standard single mode fibers at 1550 nm of D = 16 ps/(nm·km). There is no dispersion compensation in the plant. Amplified spontaneous emission (ASE) noise loading is performed in the post-amplifier. The noise figure (NF) is equal to 6 dB.

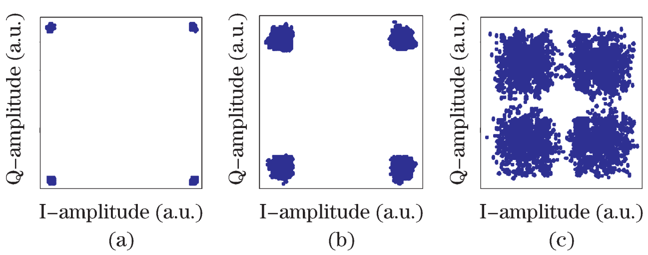

Fig. 4. Received constellation after transmission of (a) 0, (b) 50, and (c) 100 km.

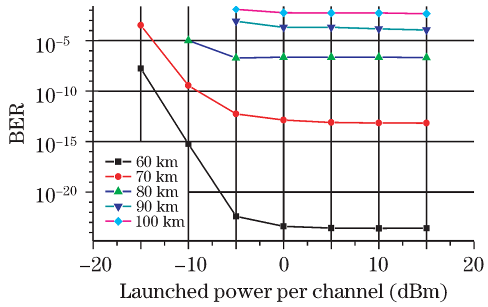

Fig. 5. BER versus launched power per channel for different span lengths.

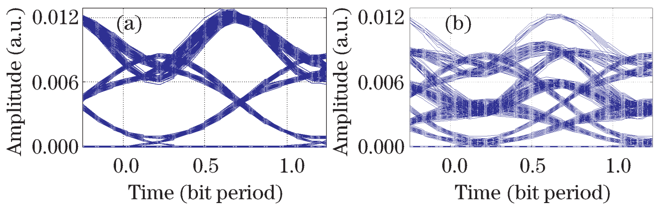

Fig. 6. Eye diagrams of (a) ch.0 and (b) ch.1.

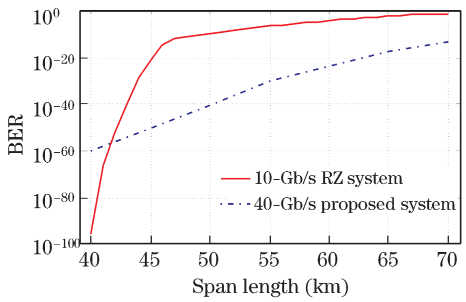

Fig. 7. BER versus span length for the RZ system and the proposed system.

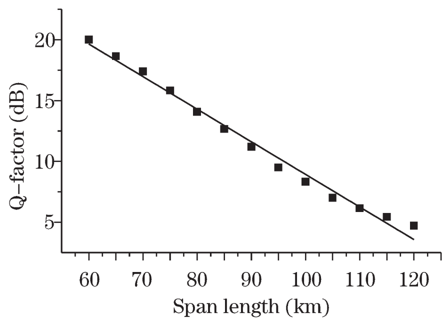

Fig. 8. Q factor versus span length for the proposed system.

At the receiver terminal, the wavelengths are demultiplexed and the signals are detected on PIN receivers. The electrical signals of eight tributaries are then filtered by fourth-order low-pass Bessel filters with a cutoff frequency of 7.5 GHz. After sampling and coefficients multiplying, FFT is performed. The received constellation can then be extracted from amplitudes of 1st and 3rd subcarriers at the outputs of FFT. Figure 4 shows the received constellation after transmission of 0, 50, and 100 km, respectively, without dispersion compensation (launched power is 10 dBm/channel).

The Q-factor of the system is calculated from $q^2 = \frac{\mu^2}{\sigma^2}$ where σ^2 is the average variance of the I or Q components of the received constellation and μ^2 is the square of the mean amplitudes of the I or Q components. The Q-factor (dB) is defined as $20\log(q)$ and the BER can be estimated as $\frac{1}{2}\mathrm{erfc}\left(\frac{q}{\sqrt{2}}\right)$[7].

The relative curves of BER and launched power per channel for different span lengths are shown in Fig. 5. As shown in Fig. 5, with the increase of launched power per channel, BER curves for different span lengths begin to be flat. The reason of this phenomenon is that when the launched power is low, the optical power at the receiver is low and the BER of the system is high. As the launched power increases, the performance of the system gets better. Furthermore, with the increase of the launched power, the optical power at receiver will reach a point (lower than the saturation point) which falls in the dynamic range of the received power. On this basis, increasing launched power has little influence on the performance of the system and the BER becomes basically unchanged. In this way, there exists a reasonable launched power for the system. When the launched power is higher than this value, little improvement on BER can be achieved by increasing the launched power.

Figure 6 shows the eye diagrams of ch.0 and ch.1 after 60-km transmission (launched power per channel is 10 dBm). As shown in Fig. 6, the eye diagrams of ch.0 and ch.1 get worse and especially the eye diagram of ch.1 deteriorates greatly. But a BER of 2.64×10^{-24} can still be obtained. This phenomenon is a proof to show that the system has a good tolerance to waveform distortion.

The BERs of the proposed system and single-channel RZ system are estimated under the same condition. In the RZ system, the transmitter is a 10-MHz-linewidth laser with a 30-dB extinction modulator driven by data with the rise time of 5 ps. The RZ receiver uses a 7.5-GHz fourth-order electrical Bessel filter. Figure 7 shows the relative curves of BER and span length. The solid curve shows the BER of a single-channel RZ system (10-Gb/s total capacity, 15-dBm launched power) for different span lengths. The dashed curve shows the BER of the proposed system (40-Gb/s total effective capacity and 15-dBm launched power per channel) for different span lengths. As shown in Fig. 7, when the span length is less than 42 km, the RZ system performs better than the proposed system. With the increase of span length, the RZ system is affected by chromatic dispersion more greatly than the proposed system. When the span length is longer than 42 km, the performance of the proposed system is superior to that of the RZ system. The curve of Q-factor versus span length of the proposed system is shown in Fig. 8. A Q factor of 9.5 can be obtained after 95-km unrepeatered transmission without dispersion compensation. With the increase of span length, the Q-factor of the system decreases almost linearly.

In conclusion, a novel structure for ULS optical transmission system has been demonstrated. In the transmission fiber, bit rate of each tributary is a quarter of that of the system. The key technology used is IFFT in combination with RZ and three-level formats in the transmission. In a purely dispersive fiber, though eye diagram deteriorates, error-free performance can still be achieved after 60-km transmission without dispersion compensation. Compared with the traditional RZ system, the proposed system performs better after long distance unrepeatered transmission. The Q-factor of the system after 95-km transmission is equal to 9.5 dB, which satisfies the forward error correction (FEC) limit. When advanced technologies are applied, ULS unrepeatered transmission can be expected.

This work was supported by the Shanghai Leading Academic Discipline Project under Grant Nos. S30108 and 08DZ2231100.

References

1. J.-X. Cai, M. Nissov, W. Anderson, M. Vaa, C. R. Davidson, D. G. Foursa, L. Liu, Y. Cai, A. J. Lucero, W. W. Patterson, P. C. Corbett, A. N. Pilipetskii, and N. S. Bergano, in *Proceedings of OFC 2006* OFD3 (2006).
2. A. J. Lucero, D. G. Foursa, D. Kovsh, M. Nissov, and A. N. Pilipetskii, in *Proceedings of OFC 2007* JThA39 (2007).
3. A. Lucero, D. G. Foursa, C. R. Davidson, M. Nissov, D. Kovsh, and A. N. Pilipetskii, in *Proceedings of OFC 2008* OTuE3 (2008).
4. H. Maeda, G. Funatsu, and A. Naka, Electron. Lett. **41,** 34 (2005).
5. J. He, L. Chen, and S. Wen, Chin. Opt. Lett. **7,** 15 (2009).
6. J. Armstrong and A. J. Lowery, Electron. Lett. **42,** 370 (2006).
7. A. J. Lowery, L. B. Du, and J. Armstrong, J. Lightwave Technol. **25,** 131 (2007).
8. J. Gao, X. Xu, Q. Chang, and Y. Su, Chin. Opt. Lett. **7,** 109 (2009).